Learning differentially shapes prefrontal and hippocampal activity patterns during classical conditioning

Jan L. Klee[1], Bryan C. Souza[1], Francesco P. Battaglia[1]

(1) Donders Institute for Brain, Cognition and Behaviour, Radboud University, Radboud University, Nijmegen

Abstract

The ability to use sensory cues to inform goal directed actions is a central element of intelligent behavior, and depends on multiple high order cortical areas. Here, we employed high-density electrophysiological recordings from the hippocampal CA1 area and the prefrontal cortex (PFC) while mice learned to respond to sensory cues with anticipatory licking. CA1 and PFC neurons undergo distinct learning dependent changes in evoked and sustained sensory cue-related activity during conditioning. At the population level, both areas maintain representations of cue identity during anticipatory behavior. In addition, reactivation of task-related neuronal assemblies during hippocampal awake Sharp-Wave Ripples (aSWR) changed quickly in CA1 within individual sessions and slowly in PFC throughout learning, and reflected reward representations in PFC and stimulus identity in CA1. Together, our results suggest that the brain tracks cue information during anticipatory behavior and that learning shapes reactivation of task-related activity patterns within the CA1-PFC circuit.

Introduction

The ability to react to sensory cues with appropriate behavioral responses confers a significant adaptive advantage. Such anticipatory behavior likely requires the interplay between a large network of cortical and subcortical brain structures, including the medial prefrontal cortex (PFC) and the CA1 area of the hippocampus (Allen et al., 2017; Steinmetz et al., 2019). Both areas have been found to respond to sensory cues and reward in various behavioral paradigms (Aronov et al., 2017; Chen et al., 2013; Starkweather et al., 2018; Taxidis et al., 2020) as well as to correlate with action planning and execution (Otis et al., 2017; Terada et al., 2017). However, a direct comparison between these two areas in the same sensory guided behavioral task has been missing and could help to tease apart how PFC and CA1 differentially respond during learning and execution of goal-directed, anticipatory behavior (Kaefer et al., 2020).

PFC has been suggested to map contextual and sensory information to appropriate actions according to flexible rules (Euston, 2012). Accordingly, PFC has been found to control the development and expression of anticipatory licking during sensory guided reward-seeking behavior (Otis et al., 2017). PFC also maintains working memory representations of sensory cues over delay periods when behavioral responses are suppressed (Funahashi et al., 1993; Goldman-Rakic, 1995). In those studies, PFC activity subsides at the moment in which the subject initiates a response. Whether this is also the case for sensory cue representations during a classical conditioning when anticipatory responses begin earlier, remains to be seen. Similar to PFC, CA1 responds to sensory cues, displays sustained activity during delay periods and is required for the learning of some forms of anticipatory behavior (Hattori et al., 2015; McEchron and Disterhoft, 1997; McEchron et al., 1999; Takehara et al., 2003). Interestingly, strong predictions can cause suppression of responses to sensory stimuli in CA1 (Rummell et al., 2016).

CA1 and PFC have also been shown to interact during awake hippocampal Sharp-Wave Ripples (aSWRs) (Jadhav et al., 2016). aSWRs have been suggested to support planning of goal directed actions mostly in the context of spatial navigation (Ólafsdóttir et al., 2018) and disruption of aSWRs leads to impairments in sensory-cue guided aversive anticipatory behavior (Nokia et al., 2012). Sensory cue representations were found to get reactivated in hippocampal and cortico-hippocampal circuits during aSWRs (Herzog et al., 2020; Rothschild et al., 2017). In addition, reactivation of cell assemblies during sleep SWRs has been hypothesized to support

65 the stabilization of task-related representations in cortical circuits during systems memory
66 consolidation (Battaglia et al., 2011; Peyrache et al., 2009). Yet, whether task related
67 information during classical conditioning is also reactivated in the CA1-PFC circuit and how
68 this changes over the course of learning is currently unknown.
69 Here, we investigate how neural activity patterns in CA1 and PFC change throughout learning
70 of sensory guided behavior, if information related to sensory cues is maintained while
71 anticipatory actions are performed, and whether task-related information is reactivated in the
72 CA1-PFC circuit. To this end, we performed electrophysiological recordings from both areas in
73 head-fixed mice while the animals performed an auditory guided trace conditioning paradigm.
74 Our findings reveal that CA1 and PFC exhibit distinct learning dependent changes in sensory
75 cue evoked activity, trial type and sensory-cue related sustained activity as well as reactivation
76 of task-related neural assemblies during aSWR.
77

78 ## Results

79 **Head-fixed mice learn to anticipate reward during appetitive auditory trace conditioning**
80 We trained head-fixed mice to associate one of two sounds (CS+ vs CS-) with a liquid reward
81 delivered after a 1-second-long, silent trace period (Figure 1 A) (Otis et al., 2017). Successful
82 learning expressed as the emergence of anticipatory licking of the animals in response to CS+
83 sounds (Figure 1 B & C). Across all animals, lick rates during the trace period were significantly
84 higher during CS+ trials after 5 days of training (Figure 1 C; Wilcoxon rank sum, $p<0.01$).
85

86 **CA1 and PFC represent reward predicting sounds with stronger evoked responses after**
87 **learning**
88 We next investigated how learning shapes neural dynamics in PFC and CA1 during learning. To
89 this end, we performed high-density silicon probe recordings from dorsal CA1 and PFC (1773
90 and 2293 cells total in CA1 and in PFC, 35 and 57 respectively per session), during the first two
91 days of training and after the animals successfully acquired the conditioning task (hereafter
92 referred to as pre and post learning) (Figure 1D, 1E and 1J). We observed that over the course
93 of learning both areas developed pronounced differences in neural activity patterns between
94 CS+ and CS- trials. Both areas displayed stronger evoked responses to CS+ compared to CS-
95 stimuli post learning and stronger sustained activity during the trace period. Yet, the polarity

of the trace period modulation, as well as the nature of pre- to post-learning changes was markedly different between CA1 and PFC.

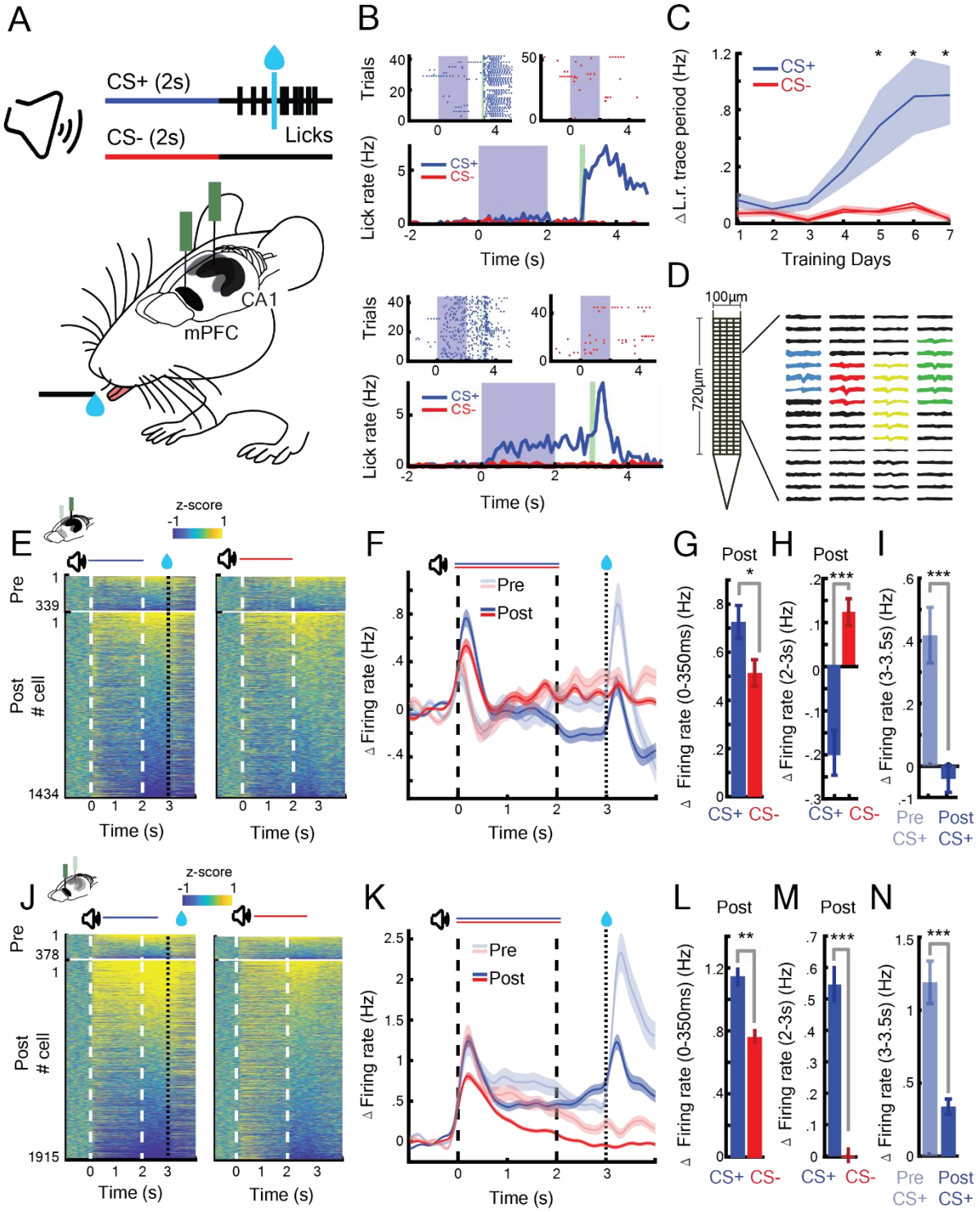

Figure 1. CA1 and PFC single cell activity shows distinct learning-dependent changes during appetitive auditory trace conditioning (AATC). A) *Schematic of AATC task and electrophysiological recordings* ***B)*** *Example post-learning training sessions of one mouse during the AATC task (dots in raster-plots represent licks, solid lines indicate average responses from respective sessions).* ***C)*** *Average change in lick rate during the trace period trial during learning for all animals (n=17) (*indicates*

sessions with a significantly higher group average licks during the trace period after CS+ sounds, Shade area represents standard error). ***D)*** *"Neuroseeker" silicon probe layout and combined spatial spike waveform patterns of 4 simultaneously recorded example neurons from CA1.* ***E)*** *Z-scored firing rates of all CA1 neurons recorded pre (top) and post (bottom) learning during CS+ and CS- trials ordered according to average trace period firing rates.* ***F)*** *Average baseline-corrected PSTHs of all recorded cells in CA1 (shade area represents SE).* ***G)*** *Average evoked change in firing rate (0-350ms post CS+/CS- onset) in CA1 (*represents Wilcoxon rank sum, p<0.05).* ***H)*** *Average trace period change in firing rate (2-3s post CS+/CS- onset) in CA1 (*** represents Wilcoxon rank sum, p<0.001).* ***I)*** *Average reward period change in firing rate (0-.5s post reward presentation for CS+ trials pre and post learning) in CA1.* ***J)*** *Z-scored firing rates of all PFC neurons recorded pre (top) and post (bottom) learning during CS+ and CS- trials ordered according to average trace period firing rates.* ***K)*** *Average baseline-corrected PSTHs of all recorded cells in PFC.* ***L)*** *Average evoked change in firing rate in PFC (** represent Wilcoxon rank sum, p<0.05 and p<0.01).* ***M)*** *Average trace period change in firing rate in PFC.* ***N)*** *Average reward period change in firing rate in PFC.*

In CA1, post-learning evoked responses to CS+ stimuli were significantly stronger than to CS- stimuli but responses to both CS+ and CS- sounds increased over the course of learning (ANOVA: trial type-learning stage interaction F(1,3268)=4.35, p=0.03, post-hoc Wilcoxon rank sum, p=.013) (Figure 1F and 1G). During the following trace period, average single cell responses in CA1 were significantly suppressed after CS+ sounds in post-learning sessions, even though a smaller group of individual cells showed sustained increases in firing rate. (Wilcoxon rank sum, p<0.001) (Figure 1H).

Similar to CA1, post-earning evoked responses in PFC to CS+ stimuli were also significantly stronger than to CS- stimuli. However, this was mostly due to a reduction in evoked responses to CS- stimuli over the course of learning rather than an increase in the responses to CS+ stimuli as in CA1 (ANOVA: trial type-learning stage interaction F(1,4416)=6.86, p=0.009, post-hoc Wilcoxon rank sum, p=.026) (Figure 1K and 1L). In contrast to CA1, single cells in PFC exhibited, on average, a strong increase in responses to CS+ trials during the trace period in post-learning sessions (Wilcoxon rank sum, p<0.001) (Figure 1M).

In addition to changes in CS evoked activity, we also observed a strong decrease in evoked activity during the reward period when comparing pre- and post-learning sessions in both CA1 (Wilcoxon rank sum, p<0.001) and PFC (Wilcoxon rank sum, p<0.001) (Figure 1I and 1N).

137 **Subset of single cells in CA1 and PFC show lick related acitivty**

138 Over the course of learning, mice start to respond to CS+ sounds with anticipatory licking.
139 Therefore, we investigated whether CA1 and PFC also exhibited time-locked activity at the
140 onset of anticipatory licking during CS+ trials. In line with previous reports showing the
141 involvement of PFC in licking behavior during appetitive trace conditioning (Otis et al., 2017),
142 we found that single cells in PFC showed increases and decreases in activity compared to pre-
143 trial baseline that were aligned to the first anticipatory lick (PFC Lick Up, n = 264, 14% of all
144 cells; PFC Lick Down, n = 208, 11% of all cells , Criterion: mean activity during -250ms - +250ms
145 around 1th lick, 1 standard deviation above pre-trial baseline) (Figure 2D). We also found that
146 a smaller population of CA1 cells responded strongly during licking (CA1 Lick-up, n = 91, 6%;
147 CA1 Lick Down, n = 170, %12) (Figure 2A).

148

149 **CA1 and PFC non-lick cells exhibit distinct patterns of trial type-specific sustained activity**

150 However, lick related activity was not the only driver of single cell modulation in the interval
151 between CS and US. After removing all cells that were classified as lick responsive from the
152 analysis, we discovered a large subset of single cells that exhibited trial type specific sustained
153 responses during the trace period in CA1 and PFC. In CA1, cells with increased activity during
154 the trace period surprisingly exhibited longer lasting (increased) responses to CS- stimuli
155 (Trace-Up, n = 444, 31%, Criterion: mean activity during trace period, 1 standard deviation
156 above pre-trial baseline in either CS+ or CS- trials) (Figure 2B and 2C (top)). On the other hand,
157 CA1 cells with decreased activity during the trace period instead showed markedly more
158 suppression after CS+ stimuli (Trace-Down, n = 675, 40%) (Figure 2B &and 2C (bottom)). This
159 pattern of reduced activity after CS+ sounds is in line with the overall suppression during the
160 trace period that we observed in the average activity in CA1 (see above Figure 1 F).

161 In PFC, single cells with increased activity during the trace period showed sustained activity
162 predominantly after CS+ sounds (Trace-Up, n = 735, 38%) (Figure 2E and 2F (top)), while PFC
163 single cells with decreased activity during the trace period, similar to CA1, also responded
164 primarily with suppression to CS+ sounds (Trace-Down, n = 736, 38%) (Figure 2E and 2F
165 (bottom)).

166

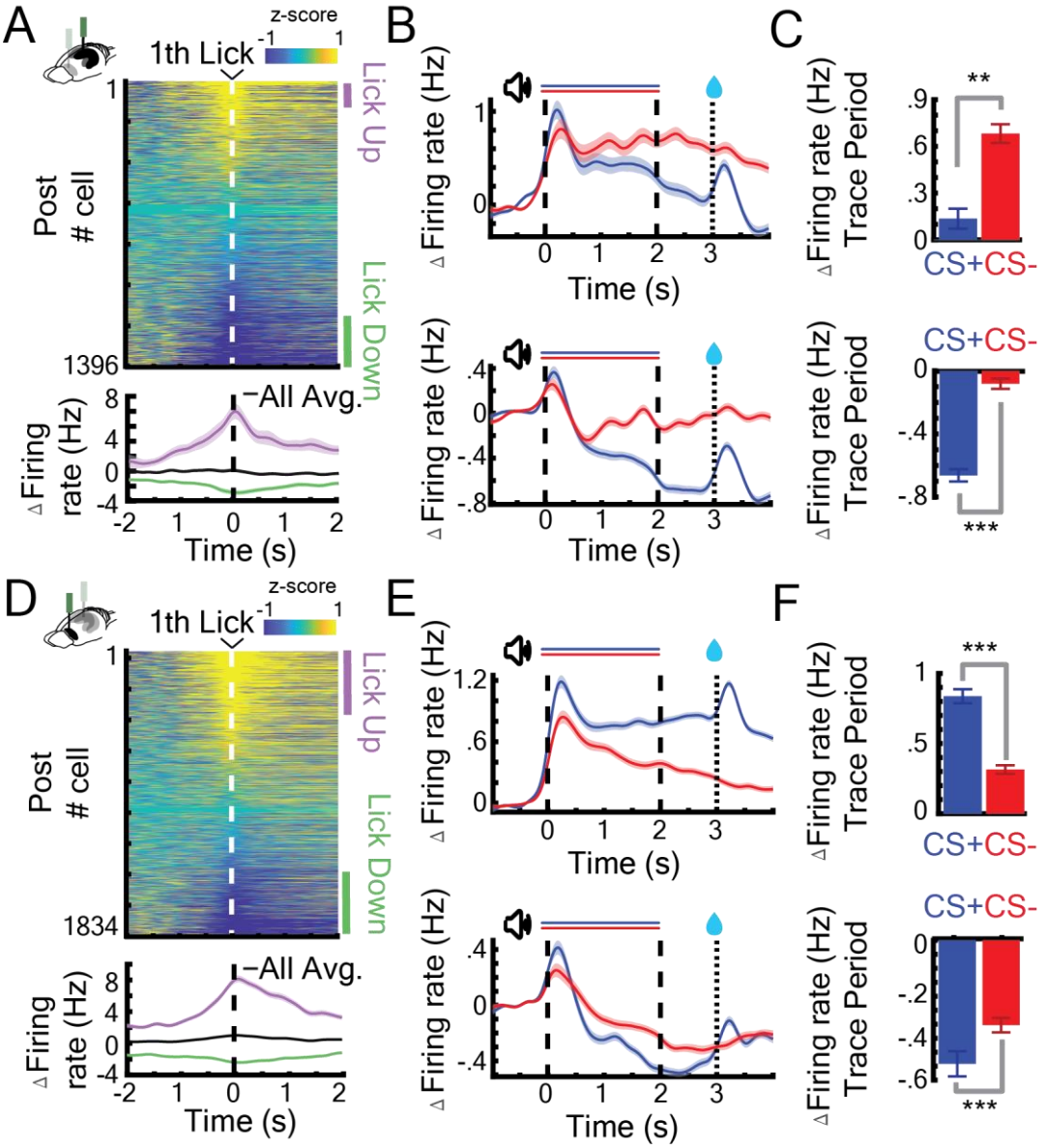

Figure 2. CA1 and PFC single cells exhibit lick evoked responses and distinct patterns of sustained activity during the AATC task. A) *Z-scored firing rates of all CA1 neurons (Top) aligned to the first lick of a lick bout (at least 3 licks/s) during CS+ trials (before reward delivery). Average change in activity of all, positively and negatively lick modulated cells (bottom). Purple and green bars indicate Lick Up and Lick Down cells.* ***B)*** *Average baseline-corrected PSTHs of all Trace-up (Top) and Trace-Down (Bottom) non-lick neurons post-learning for CA1 (Trace up, n=444; Trace Down, n=675).* ***C)*** *Average mean change in firing rate during the trace period of the same Trace-Up neurons (Top) and Trace-Down neurons (bottom) for CA1 (** & *** represent Wilcoxon rank sum, p<0.01 and p<0.001 respectively).* ***D)*** *Z-scored firing rates of all PFC neurons (Top) aligned to the first lick of a lick bout (at least 3 licks/s) during CS+ trials (before reward delivery). Average change in activity of all, positively and negatively lick modulated cells (bottom).* ***E)*** *Average baseline-corrected PSTHs of all Trace-up (Top) and Trace-Down (Bottom) non-lick neurons post-learning for PFC (Trace up, n=736; Trace Down, n=734).* ***F)*** *Average*

mean change in firing rate during the trace period of the same Trace-Up neurons (Top) and Trace-Down neurons (bottom) for PFC.

CA1 and PFC population activity distinguishes between rewarded and unrewarded trials during the trace period

Because individual cells in CA1 and PFC exhibited sustained activity during the trace period, we hypothesized that these responses might be part of a broader CA1 and PFC population code to maintain a representation of trial identity between CS and US (i.e. in the trace period, in which there is no on-going stimulus). To test this, we first computed the binned population rate vectors for all simultaneously recorded non-lick cells in both areas during CS+ and CS- trials on a session by session basis. We next calculated the Euclidean distance between the population rate vector trajectories of the two stimuli (see Figure 3A and 3C for trajectory examples), and used this metric as a proxy of the similarity of population responses over time. We found that in post-learning sessions, the population rate vector distance increased after stimulus onset and persists to be significantly different from baseline during the trace period in CA1 (Wilcoxon sign rank, $p<0.001$) and PFC (Wilcoxon sign rank, $p<0.001$), indicating that both areas maintain trial type specific information at the population level. Non-lick cell population rate vector distance did not correlate with lick activity or movement of the animals in CA1 ($n=36$, Population Vector Distance vs. Licks: correlation coefficient =.14, $p=.42$; Population Vector Distance vs movement: correlation coefficient = .03, $p= .85$; Figure S1C) or PFC ($n=38$, Population Vector Distance vs. Licks: correlation coefficient =-.1, $p=.52$; Population Vector Distance vs movement: correlation coefficient = -.04, $p= .74$; Figure S1D).

To verify that both areas maintain CS type specific information on a trial by trial basis, we next trained a support vector machine classifier on the firing rates of simultaneously recorded non-lick cells during the trace period from either CA1 or mPFC. We were able to predict the preceding trials stimulus identity significantly above chance level in CA1 (mean performance, 62% correct, Wilcoxon sign rank $p<0.001$; Figure 3C) and PFC (mean performance, 76% correct, Wilcoxon sign rank $p<0.001$; Figure 3F).

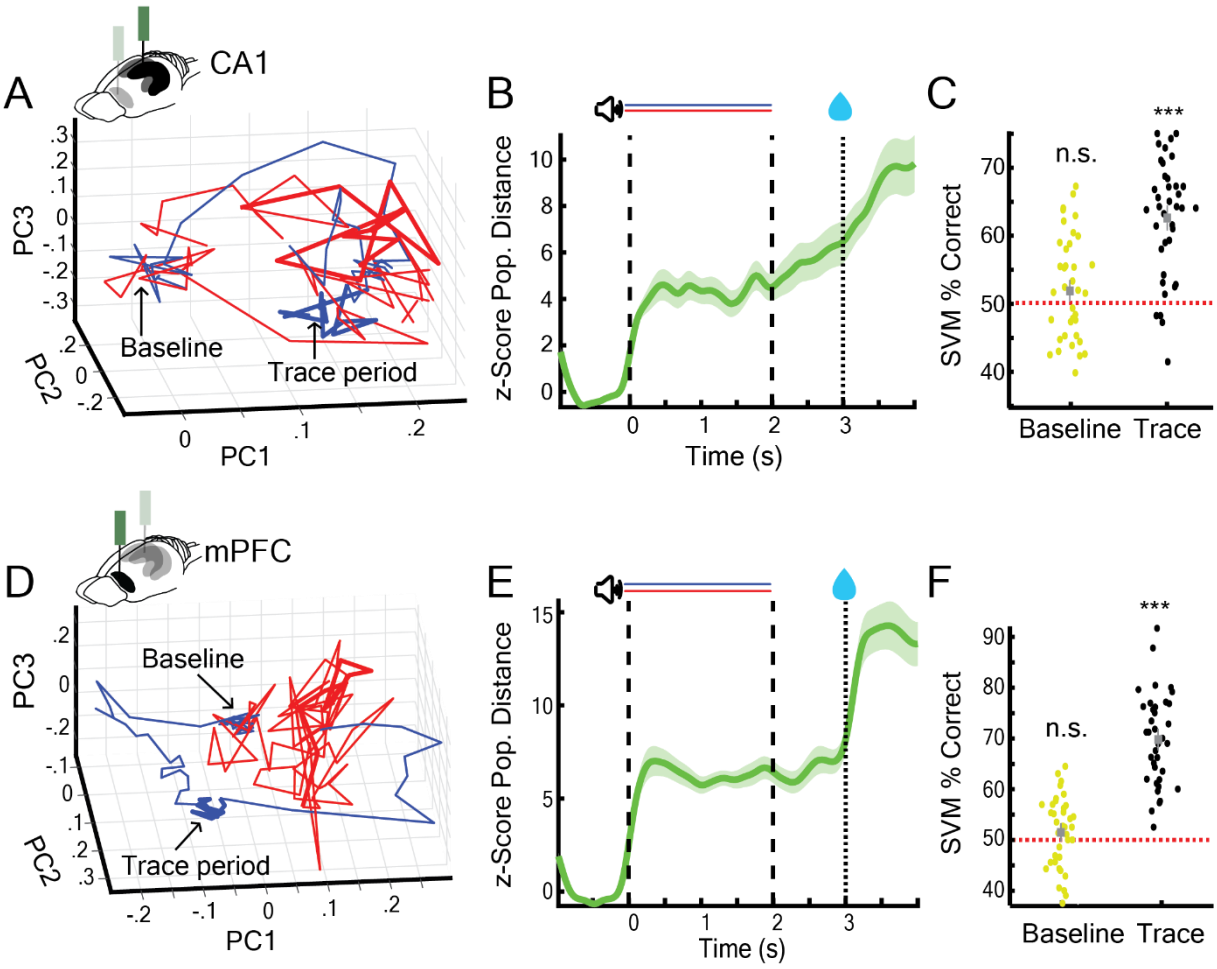

Figure 3. CA1 and PFC non-lick cell population activity encode trial identity during trace period. A) *Example of average non-lick cell population rate vector trajectories for one session in CA1 (CS+ (blue) and CS- (red)). Averages plotted along first 3 principal components (Baseline period: blob on the left, trace period thicker lines on the right).* ***B)*** *Average z-scored Euclidean-distance between CS+ and CS- non-lick cell population rate vector trajectories during AATC task for CA1 (n=36).* ***C)*** *Support vector machine classification of trial identity by average baseline (-1s-0) and trace period (2-3s) activity of non-lick cells in CA1 (n=36) (*** indicate Wilcoxon sign rank p<0.001).* ***D)*** *Example of average non-lick cell population rate vector trajectory for one session in PFC.* ***E)*** *Average z-scored Euclidean-distance between CS+ and CS- non-lick cell population rate vector trajectories for PFC (n=38).* ***F)*** *Support vector machine classification of trial identity by average baseline (-1s-0) and trace period (2-3s) activity of non-lick cells in PFC (n=38).*

Ca1 and PFC population activity maintains stimulus-specific information during the trace period and reward consumption

Having identified trial type specific population responses in CA1 and PFC during the stimulus free trace period, we next asked whether these sustained responses could carry information

225 about the preceding CS+ sound. To answer this question, we trained a new set of animals on
226 a modified version of the conditioning task which included a second CS+ sound. This modified
227 task allowed us to contrast neural responses to two different CS+ sounds which were
228 associated with the same behavioral response pattern and reward contingencies (Figure 4A
229 and 4B). We hypothesized that if sustained neural responses are purely related to reward
230 prediction or motor output they should be similar between CS+ trials with different cue sound
231 identities. On the other hand, if sustained responses are related to sound specific information,
232 the activity patterns should differ.
233 As in the original task, we found on the single cell level that short-latency evoked responses
234 to CS+ sounds are significantly stronger compared to CS- sounds in CA1 and PFC (Figure 4C
235 and 4F). Grant average trace period responses in CA1 did not show the suppression to CS+
236 stimuli which we found in the original version of the task. However, we did find the same
237 pattern of CS+ specific suppression after removing lick-modulated cells from the analysis and
238 further separated single cell responses into Trace-Up and Trace-Down cells (Figure S2B and
239 S2C). Similarly, in PFC the removal of lick-modulated cells and further separation of single cell
240 responses in Trace-Up and Trace-Down cells revealed CS+ specific increases in activity during
241 the trace period (Figure S2D and S2E).
242 In order to investigate the presence of sound specific information during the trace period, we
243 then again computed the binned population rate vectors and their Euclidian distance over
244 time for all simultaneously recorded non-lick cells in both areas, but this time focused our
245 analysis on comparing the similarity between CS+a and CS+b trials. This analysis revealed
246 significant differences in population activity during and after CS+a and CS+b sound
247 presentation in CA1 (Wilcoxon sign rank, $p<0.001$; Figure 4D & 4E) and PFC (Wilcoxon sign rank
248 $p<0.001$; Figure 4G and 4H). This indicates that both areas maintain a representation of
249 stimulus identity during the trace period, while the animals display anticipatory licking as well
250 as during reward consumption (i.e., independent of the licking response).
251
252
253

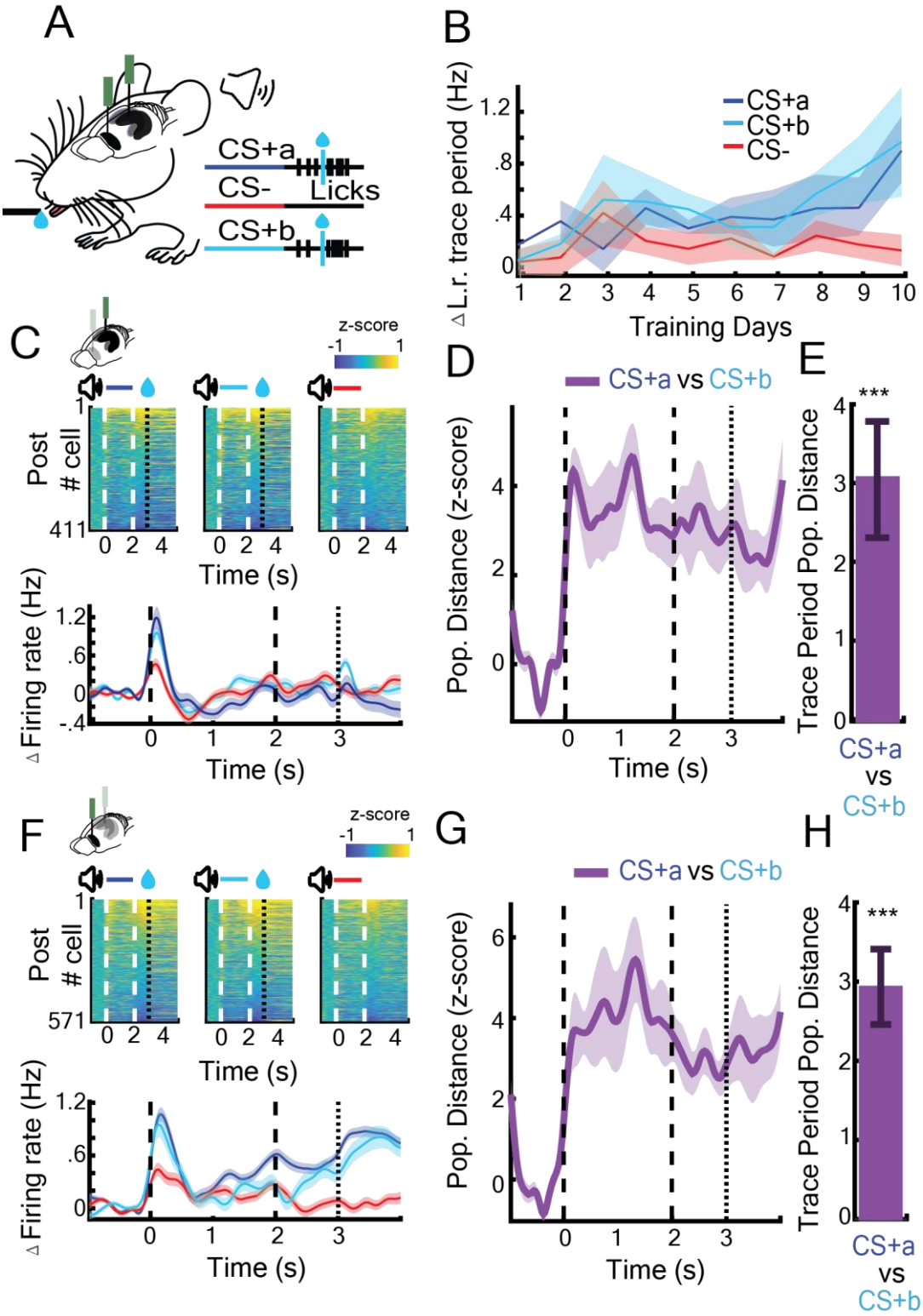

Figure 4. **CA1 and PFC non-lick cell population activity maintains stimulus-specific information during the trace period.** ***A)*** *Schematic representation of the modified version of the appetitive trace-conditioning paradigm including 2 CS+ stimuli (AATC2R).* ***B)*** *Average change in lick rate during the trace period in all 3 trial types during learning for all animals (n=5) (Shade area represents the standard error).* ***C)*** *Z-scored firing rates of all CA1 neurons recorded post-learning during CS+ a, CS+ b and CS- trials ordered according to trace period activity (top). Average baseline-corrected PSTHs of the same*

neurons (bottom) ***D)*** *Average z-scored Euclidean-distance between CS+a and CS+b non-lick cell population rate vector trajectories during AATC2R task for CA1 (B) (n=22).* ***E)*** *Average z-scored Euclidean-distance between CS+a and CS+b non-lick cell population rate vector trajectories during the trace period for CA1 (*** represent Wilcoxon sign rank, p<0.001).* ***F)*** *Z-scored firing rates of all PFC neurons recorded post-learning during CS+ a, CS+ b and CS- trials ordered according to trace period activity (top). Average baseline-corrected PSTHs of the same neurons (bottom).* ***G)*** *Average z-scored Euclidean-distance between CS+a and CS+b non-lick cell population rate vector trajectories during AATC2R task for PFC (n=22).* ***H)*** *Average z-scored Euclidean-distance between CS+a and CS+b non-lick cell population rate vector trajectories during the trace period for PFC.*

Task-related neuronal assemblies are more strongly reactivated in PFC during aSWR after learning

Learning-dependent reorganization of cortical circuits during memory consolidation has previously been linked to activity during hippocampal SWRs (Peyrache et al., 2009). aSWRs have additionally been implicated in the planning of goal-directed behavior (Ólafsdóttir et al., 2018). Therefore, we wondered if we could find evidence for reactivation of task-related neural assemblies during aSWRs occurring during inter-trial intervals of the conditioning task. To test this, we first detected the presence of neuronal cell assemblies in concatenated trial activity (Lopes-dos-Santos et al., 2013) and then checked the reactivation strength of these task related assemblies during aSWRs in CA1 and PFC. We found that reactivation of task-related assemblies in PFC increases significantly over the course of learning during hippocampal aSWRs (Figure 5A & 5B) (Wilcoxon rank sum test; $p<0.05$). In CA1, on the other hand, reactivation strength remained constant from pre to post-learning sessions ($p=0.337$).

Task-related assembly reactivation strength increases during individual sessions in CA1

We next analyzed how reactivation strength changed over time within individual sessions. We found that in CA1 assembly reactivation strength increases gradually over the course of individual pre-learning sessions for assemblies that are positively modulated (reactivation+) as well as for assemblies that are negatively modulated (reactivation-) during aSWRs (Figure 5C). This effect was also present in post-learning sessions for the reactivation+ assemblies (One-way ANOVA; CA1 pre+: $p<0.01$, pre-: $p=0.05$, pos+: $p<0.001$, post-: n.s.). In contrast to CA1, assembly reactivation strength in PFC remained generally constant over the course of individual sessions (Figure 5C).

Finally, we sought to determine what type of task specific information the most strongly SWR-reactivated assemblies represent during the conditioning task in post learning sessions. In CA1, we found that the 25% most reactivated assemblies are suppressed during the trace and reward period after CS+ trials compared to CS- trials, similar to what we observed on the single cell level (Figure 5D) (Wilcoxon signed-rank; $p<0.001$). In PFC, on the other hand, the 25% most reactivated assemblies responded strongly during the reward period (Figure 5E) (t-test, compared to pre-trial baseline; $p<0.05$). Those effects were not observed for the 25% least reactivated cells.

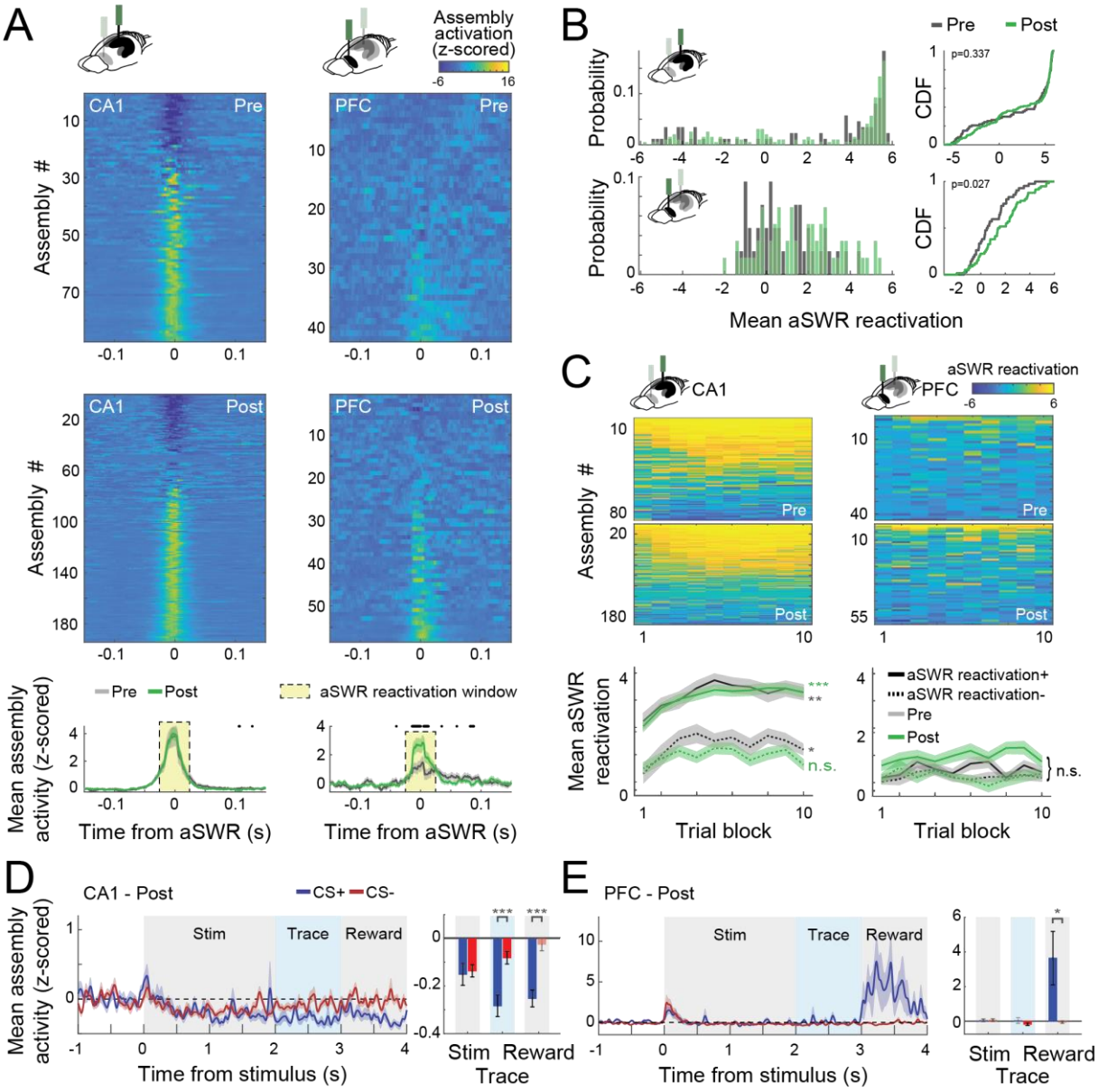

305 ***Figure 5. CA1 and PFC cell assemblies show different aSWR reactivation dynamics. A)*** *Average (z-*
306 *scored) assembly activation triggered by aSWR occurring in the inter-trial intervals for CA1 and PFC,*
307 *Pre and Post learning sessions (Top). Mean aSWR-triggered activation over all the assemblies for Pre*
308 *and Post sessions for each area. Shaded areas represent the standard error of the mean. Black dots*
309 *represent windows in which Pre and Post assembly activity were statistically different (Wilcoxon rank*
310 *sum test; p<0.05). Notice the higher aSWR triggered activation of assemblies in PFC in Post sessions.* ***B)***
311 *Histogram (left) and cumulative distribution function (CDF; right) of the mean assembly activity on the*
312 *reactivation window denoted in A. P-values refer to a two-sample Kolmogorov-Smirnov test between*
313 *Pre and Post distributions.* ***C)*** *Average aSWR reactivation of each assembly per session (Top). Sessions*
314 *were divided into 10 blocks of equal trial length. Mean aSWR reactivation of all positively*
315 *(reactivation+) and negatively (reactivation-) reactivated assemblies. Asterisks refer to one-way*
316 *ANOVA performed with all trial blocks of one area/learning condition (n.s.: non-significant; *p<0.05;*
317 ***p<0.01; ***p<0.001) and shaded areas represent SEM. Note the evident increase in CA1 aSWR*
318 *assembly reactivation across the session in both Pre and Post sessions for positively modulated*
319 *assemblies (reactivation+).* ***D)*** *Mean (z-scored) assembly activity triggered by the stimulus onset for the*
320 *25% most strongly aSWR-reactivated assemblies in CA1 (Left). Average of the traces over each trial*
321 *period is shown for CS+ and CS- (Right). Notice the initial decrease of assembly acitivty in CA1 during*
322 *the stimulus and the posterior separation between CS+ and CS-.* ***E)*** *The same as in D, but for PFC*
323 *assemblies. Note the difference between CS+ and CS-assembly activity during the reward period.*
324 *Asterisks refer to a Wilcoxon signed-rank test comparing CS+ and CS- (*p<0.05; **p<0.01; ***p<0.001).*
325 *Error bars refer to SEM and darker bars denote mean assembly activity significantly different from zero*
326 *(p<0.05; t-test).*
327

328 ## Discussion

329 We found that CA1 and PFC undergo distinct learning dependent changes in evoked and trace
330 period activity while mice learn to respond to sensory cues with anticipatory licking (Figure
331 1E-1N). In both areas, reward predicting sounds lead to stronger evoked responses compared
332 to control sounds after learning. Furthermore, both areas displayed long-lasting trace period
333 responses with a similar time course. Yet, while CA1 responds with mostly sustained
334 suppression during the trace period after reward-predicting CS+ sounds, the activity in PFC is
335 thereby mostly elevated. By comparing trace responses on the population level, we show that
336 both areas maintain information about trial type (Figure 3) and preceding sensory cue identity
337 (Figure 4) even during anticipatory licking and reward consumption. Lastly, we found that task
338 related assemblies are reactivated during aSWR. In PFC, the reactivation of such assemblies

339 increased over the course of learning as behavioral responses stabilized. In contrast, in CA1,
340 assembly reactivation showed an increase during individual sessions for both positively and
341 negatively modulated assemblies, although the effect disappears after learning for negatively
342 modulated assemblies.
343 PFC activity has previously been shown to control the expression of anticipatory licking (Otis
344 et al., 2017) and CA1 has long been indicated in learning of anticipatory aversive responses
345 during eye-blink trace conditioning (McEchron et al., 1999; Takehara et al., 2003). Given the
346 importance of CA1 and PFC for anticipatory behavior, the differences in learning dependent
347 reorganization of sound evoked responses between both areas that we find in this study are
348 particularly noteworthy. In early training sessions, PFC displays strong and long lasting evoked
349 responses to novel CS+ and CS- sounds (Figure 1K). These slowly decaying responses would be
350 ideally suited to create a link to behaviorally relevant events, i.e. reward delivery, that happen
351 after CS offset. In PFC, evoked and trace period responses to CS- sounds decrease over the
352 course of learning (Figure 1K), indicating that PFC primarily maintains representations of novel
353 sounds if they are linked to a subsequent reward. In contrast, in CA1 evoked responses to both
354 novel sounds become stronger and longer lasting over the course of learning (Figure 1F)
355 suggesting that the hippocampus plays a role in processing familiar stimuli even if they are not
356 linked to a subsequent reward. In line with this idea, we found a small group of cells in CA1
357 that, in fact, show long lasting positively modulated trace period responses after learning in
358 response to CS- sounds (Figure 2B).
359 However, the predominant response pattern in CA1 after learning is sustained suppression
360 during the trace period after reward predicting CS+ sounds. Responses to predictable sensory
361 events have previously been shown to be strongly suppressed in CA1 (Rummell et al., 2016).
362 Similarly, well predicted evoked responses to reward during post learning sessions are
363 suppressed in CA1 in our study. Sustained inhibition after reward predicting cues has been
364 suggested to be important for the encoding of prediction error signals in the brain and are
365 found e.g. in the ventral tegmental area (Cohen et al., 2012). The suppression within the CA1
366 might therefore be part of the brain's reward prediction system (Lisman and Grace, 2005).
367 Despite the fact that CA1 exhibits mostly trace period suppression and PFC displays mostly
368 trace period increases in activity to reward predicting sensory cues, we were able to show that
369 in both areas, different rewarded cues also cause different patterns of sustained population
370 activity (Figure 4D and 4G). Both areas therefore maintain a representation of cue identity

371 during the trace period. Maintaining cue information might be crucial in situations in which
372 cue reward contingencies change. Maintaining a representation of cue identity would allow
373 flexible relearning of cue reward contingencies independent of the operant component, i.e.
374 when licking is still the correct behavioral response but only after one of the two CS+ sounds.
375 However, whether cue identity is maintained in coordinated activity patterns between both
376 areas and how changing cue contingencies affects the CA1-PFC circuit would need to be
377 explored in future experiments.
378 Lastly, we found that cell assemblies in CA1 and PFC that are responsive during classical
379 conditioning also strongly activate during awake hippocampal Sharp-Wave Ripples (aSWRs).
380 Coordinated activity in CA1 and PFC has previously been found to be elevated during aSWRs
381 and to change over the course of learning of a spatial memory task (Jadhav et al., 2016; Tang
382 et al., 2017) but physiological evidence for reactivation of neural assembly patterns during
383 aSWRs in a non-spatial task had been missing. Our data now provides this missing link and
384 adds to the notion that reactivation of task-related patterns of neural activity during aSWRs
385 plays a general role during learning and action planning (Joo and Frank, 2018; Ólafsdóttir et
386 al., 2018). Notably, we observed a fast increase in reactivation strength within CA1 as
387 individual training sessions progressed and a slow increase in reactivation strength in PFC from
388 pre-learning to post-learning sessions. This is well in line with the idea that both areas support
389 learning on different timescales, with the hippocampus adapting fast to new experiences and
390 the prefrontal cortex adapting more slowly to behaviorally important variables that remain
391 stable over time (McClelland et al., 1995; Takehara-Nishiuchi and McNaughton, 2008;
392 Takehara et al., 2003). Also, CA1 assemblies could be negatively modulated during aSWRs,
393 possibly contributing to the destabilization of those representations as previously found for
394 hippocampal place cells (Roux et al., 2017). The inactivated assemblies were modulated along
395 the session in pre but not in post learning sessions, suggesting that they were specifically
396 involved in the initial stages of learning.
397 Moreover, aSWRs-reactivated assemblies in PFC strongly encode reward during the task and
398 strongly aSWRs-reactivated assemblies in CA1 exhibited long lasting suppression to CS+
399 stimuli. Together with the decrease in CA1 activity during the trace period which we observed
400 on the single cell level, those results support the idea that the hippocampus might contribute
401 to learning through a mechanism based on inhibition of specific assemblies (Lovett-Barron et

402 al., 2014).In this sense, aSWRs would help to stabilize/destabilize particular representations
403 in the hippocampus and extra hippocampal areas like PFC during learning.
404

405 Material and Methods

406 Animals

407 For this experiment, we used a total of 22 male C57/Bl6j mice. The animals were obtained at
408 10-13 months of age from Charles River Laboratory and all experiments were performed
409 within two months after delivery. 7 animals were used for silicon probe recordings from dorsal
410 hippocampus area CA1, 6 animals were used for recordings from PFC and an additional 4
411 animals were used for combined silicon probe recordings from CA1 and PFC during the AATC
412 task. 5 additional animals were used for combined silicon probe records from CA1 and PFC
413 during a modified version of the AATC task with 2 rewarded sounds (AATC2R). All animals were
414 group housed until the first surgery after which they were individually housed to prevent
415 damage to the implants. Throughout the experiment the animals were maintained on a
416 reversed 12-hour light/dark cycle and received food and water ad libitum until we introduced
417 food restriction two days after the first surgery. All experiments were performed during the
418 dark period. This study was approved by the Central Commissie Dierproeven (CCD) and
419 conducted in accordance with the Experiments on Animals Act and the European Directive
420 2010/63/EU on animal research.
421

422 Surgical preparation for head-fixed electrophysiological recordings

423 Animals were anesthetized using isoflurane (1–2%) and placed in a stereotaxic frame. At the
424 onset of anesthesia, all mice received subcutaneous injections of carprofen (5 mg/kg) as well
425 as a subcutaneous lidocaine injection through the scalp. The animals' temperature was
426 maintained for the duration of the surgical procedure using a heating blanket. Anesthesia
427 levels were monitored throughout the surgery and the concentration of isoflurane was
428 adjusted so that a breathing rate was kept constant at around 1.8 Hz. We exposed the skull
429 and inserted a skull screw over the cerebellum to serve as combined reference and ground for
430 electrophysiological recordings. We then placed a custom made, circular head-plate for head-
431 fixation evenly on the skull and fixated it with dental cement (Super-Bond C&B). For CA1
432 recordings, a craniotomy was performed over the left hippocampus -2.3 mm posterior and
433 +1.5 mm lateral to Bregma and for PFC recordings a craniotomy was performed over left

434 frontal cortex at +1.78mm anterior and +.4mm lateral to Bregma. The exposed skull was
435 covered with a silicon elastomer (Body Double Fast, Smooth-on) until the first recording. All
436 mice were given at least 2 days to recover from the surgery.
437
438 **Head-fixed virtual reality setup**
439 The head-fixed virtual reality setup consisted of two rods that were screwed onto either side
440 of the implanted head-plate and fixated the mice on top of an air-supported spherical
441 treadmill. The motion of the treadmill was recorded using an optical mouse and transformed
442 into movement along a virtual linear track designed with the Blender rendering software. The
443 virtual track was then projected through a mirror into a spherical screen surrounding the
444 head-fixed animal on the treadmill (Schmidt-Hieber and Häusser, 2013) (
445 https://github.com/neurodroid/gnoom). While in head-fixation the animals received soy milk
446 as reward which was delivered through a plastic spout that was positioned .5cm anterior to
447 the lower lip. Licks were detected with an infrared beam-break sensor that was positioned
448 right in front of the spout.
449 All animals were slowly habituated to head-fixation by placing them in the setup for at least 2
450 days of 3x10 minute sessions during which they received about 50 rewards, totaling to about
451 .2ml of soy milk. During the habituation, we started to food restrict the animals to around 90%
452 of initial bodyweight to motivate better task performance.
453 In all cases, the food restricted animals started to lick off the soymilk reward reliably within
454 the first 6 habituation sessions.
455
456 **Behavioral training**
457 The AATC task required the animals to associate a 2-second-long CS+ sound with a droplet of
458 soymilk reward (~5 microliter), delivered after 1 second of silence, the so called “trace period”
459 while ignoring a CS- control sound. We interleaved the CS presentations randomly every 30-
460 45 seconds. For the two sounds, we choose a 3000 kHz continues pure tone and a 7000 kHz
461 tone pulsating at 10hz. We counter-balanced the CS+ and CS- sounds evenly between animals
462 throughout the experiment.
463 For The AATC2R task, we interleaved the CS+a & CS+b and CS- sound presentations randomly
464 every 30-45 seconds. We choose a 3000 kHz continues pure tone and a 7000 kHz pure tone as
465 CS+(a) and CS+(b) respectively and a 5000khz continues pure tone as the CS- stimulus. We

466 counter-balanced the CS+a and CS+b sounds evenly between animals throughout the
467 experiment but kept the CS- sound constant.
468 As the main behavioral outcome measure, we detected the licks of the animals with an
469 infrared beam-break sensor that was mounted in front of the reward spout. Each training
470 session ended as soon as the animals received 50 rewards. We repeated the experiment for
471 at least 10 days.
472 During these behavioral training sessions, the head-fixed animals could freely run on the linear
473 track in the virtual reality which was otherwise not correlated with the AATC or AATC2R tasks.
474 We performed acute silicon probe recordings from the dorsal CA1 area and/or PFC of head-
475 fixed mice during first 2 days of the AATC task as well as from day 6 onwards for as long as we
476 were able to achieve stable recordings. We then classified recording sessions from the first 2
477 days of training as pre-learning (Pre) and recording sessions from day 6 onwards and with a
478 significant increase in anticipatory licks as post-learning (Post). We only recorded during post-
479 learning sessions during the AATC2R task.
480
481 **Acute electrophysiological recordings during AATC and AATCR2 tasks**
482 At the start of each recording session, we placed the mice in head-fixation and removed the
483 silicon elastomer cover to expose the skull. We then used a micromanipulator (Thorlabs) to
484 acutely insert a 128 channel silicon probe into the middle of the previously prepared
485 craniotomy above PFC and/or CA1. For PFC recordings, we then slowly lowered the recording
486 electrode to -2.0mm ventral to Bregma. For CA1 recordings, we continuously monitored the
487 local field potential (1-600Hz), ripple frequency signal (150-300Hz) and spiking activity (600-
488 2000Hz) during the insertion process and tried to positioned our electrode in a way that the
489 strongest ripple amplitude and spiking activity was 200-250µm from the base of the probe
490 and 470-520µm from the tip. In this way, we were able to cover most of dorso-ventral extend
491 of CA1 with our recording electrode.
492 Electrophysiological signals were filtered between 1 and 6000 Hz, digitized at 30 kHz using 2
493 64 channel digitizing heads-stages (RHD2164 Amplifier Board, Intan Technologies) and
494 acquired with an open-ephys recording system. After each recording session, we retracted the
495 silicon probe and placed a new silicon cover on the skull before releasing the animals back to
496 their respective home cages.
497

498 **Behavioral Data Analysis**

499 For every training session and each animal, we compared the change in lick-rate between CS+
500 vs CS- trials. In short, for each trial we took the sum of all licks during the trace period and
501 subtracted the sum of all licks during the baseline period (-1s to onset of CS). We then
502 computed a T-test between the change in lick rate for all CS+ vs all CS- trials and defined the
503 animal to have learned (post-learning sessions) if this comparison showed a significant
504 difference in lick rate between the two conditions. For analysis of the AATC2R task, we defined
505 the animal to have learned (post-learning sessions) if the average trace period lick rate for
506 both CS+ stimuli was significantly higher than for the CS- stimulus.

507

508 **Neural Data Analysis**

509 To identify single unit activity, the raw voltage signal was automatically spike sorted with
510 Kilosort (Pachitariu et al., 2016) (https://github.com/cortex-lab/Kilosort) and then manually
511 inspected and curated with the 'phy' gui (https://github.com/kwikteam/phy). All following
512 analysis was performed using custom written Matlab scripts.

513

514 **Single Cell responses**

515 For each unit, we binned the single cell spiking data (25ms), smoothed the data with Gaussian-
516 weighted moving average filter (25 Bins) and computed the Peri-Stimulus-Time-Histograms
517 (PSTH) for CS+ and CS- trails.

518 To assess evoked responses to CS+ and CS- we calculated the baseline (-1000ms-0ms)
519 corrected mean firing rates in the first 350ms (post-learning CS) post stimulus interval for each
520 cell and compared population responses in this time window.

521 To assess lick related activity, we first defined lick onset as the first lick after CS+ sound onset
522 but before reward delivery that was followed by at least 3 licks within the next second. We
523 then defined single cells to be trace responsive if the average firing rate during the time
524 window around the 1th lick (-250ms to +250ms) was increased by at least 1 standard deviation
525 or decreased by at least 1 standard deviation from pre-trial baseline (-1000 - CS+ onset)

526 To assess trace period activity, we defined single cells to be trace responsive if the average
527 firing rate during the 1 second trace period increased by at least 1 standard deviation or
528 decreased by at least 1 standard deviation from baseline during either CS+ or CS- trials.

529 To quantify group differences, we performed ANOVA with independent factors stimulus type
530 (CS+ vs CS-) and learning stage (pre vs post learning) using average baseline corrected
531 sustained responses during the trace period.
532 For analysis of learning dependent changes in reward evoked activity, we calculated the
533 baseline (-1000 – CS+ onset) corrected mean firing rates during the reward response window
534 (reward delivery- reward delivery+500ms).
535
536 **Population rate vector analysis**
537 To analyze the CA1 and PFC population response during the trace period, we first computed
538 the average CS+ and CS- PSTHs for all simultaneously recorded non-lick cells in 25ms bins for
539 every session and smoothed the data with Gaussian-weighted moving average filter (25 bins).
540 For visualization purposes, we then computed the first 3 principal components of the resulting
541 matrices CS+ and CS- PSTHs and plotted the resulting 3 dimensional vectors. To quantify the
542 difference in population activity between CS+ and CS- trials, we calculated the Euclidean
543 distance between CS+ and CS- in n-dimensional space (n=number of simultaneously recorded
544 non-lick cells) for each bin and averaged across sessions. We repeated the same procedure to
545 compare responses to CS+a and CS+b sounds during the AATC2R task.
546 In order to predict trial identity by trace period population firing rates using a support vector
547 machine classifier, we first calculated the trial by trial firing rates for all simultaneously
548 recorded cells during the trace period. We then split all trials of a single recording session into
549 20 equal partitions and used 19 of these partitions to train the support vector machine
550 classifier (fitcsvm function, MATLAB). We then tested the classifier performance on the 20th
551 partition and repeated this process for all other partitions (20fold cross validation). Classifier
552 performance above chance was determined by comparing the average prediction accuracy
553 across all sessions against chance level using a Wilcoxon sign rank test.
554
555 **Reactivation during awake Sharp-Wave Ripples**
556 In order to detected awake Sharp-Wave Ripples during the inter-trial periods of the AATC task,
557 we first filtered the local field potential at the top half of our recording electrode (16 channels
558 in total, 1 channel at each depth, 320µm spread around CA1 cell layer) between 150-300Hz
559 and used common average referencing to exclude artefacts affecting all channels. We then
560 identified the recording depth with the strongest average ripple power and used the ripple

band signal on this channel for further analysis. For each recording session, we visually inspected the ripple band signal and manually set a low-cut threshold for ripple detection (100 µV in most cases) and a high-cut threshold for artefact rejection (400µV in most cases). We furthermore, excluded threshold crossings within 200ms of each other as well as within 200ms of any licking activity.

To compute task related cell assemblies in CA1 and PFC, we first binned the spikes of each trial (-1 to 4 s from stimulus onset) into 20 ms bins. Then, we used independent component analysis (ICA) to find the co-activation patterns as described previously (Lopes-dos-Santos et al., 2013). The number of assemblies was defined by the eigenvalues of the cross-correlation matrix that were above the analytical Marcenko Pastur distribution (Lopes-dos-Santos et al., 2013). We then projected the neural activity onto each of the assembly patterns (using the same 20 ms bins, with overlap) and computed the mean assembly activity triggered by the stimulus, animal licks and hippocampal SWR, normalizing it with the z-score transformation. Normalization was done using the z-score transformation, which in the case of stimulus-triggered assembly activity only used pre-stimulus period (of both CS+ and CS-) as baseline (-1000 - 0 s). At last, we defined the assembly reactivation window on SWR as the average z-scored assembly activity in the 50 ms window centered on the aSWR. We then divided each session in 10 equally long trial blocks, and investigated the reactivation strength of positively (reactivation+) and negatively (reactivation-) modulated assemblies over the course of the session. Statistical comparisons between pre and post (normalized) mean assembly activity was done using a Wilcoxon rank sum test, while comparisons of reactivation within a session was done using a one-way ANOVA. In Figure 5D-E traces were smoothed using a 100 ms Gaussian window. Comparisons between CS+ and CS- stimuli were done using a Wilcoxon signed-rank test, while comparisons with baseline (pre-stimulus period) were done using a t-test.

Acknowledgments

Funding was provided by a German Studiesstiftung fellowship to JK, by the Dutch NWA “Bio-Art” project (to FPB), and by the NWO Top-grant no. 612.001.853 (to FPB)

Competing interests

No competing interests declared.

593 **References**

594 Allen, W.E., Kauvar, I. V., Chen, M.Z., Richman, E.B., Yang, S.J., Chan, K., Gradinaru, V.,
595 Deverman, B.E., Luo, L., and Deisseroth, K. (2017). Global Representations of Goal-Directed
596 Behavior in Distinct Cell Types of Mouse Neocortex. Neuron *94*, 891-907.e6.
597 Aronov, D., Nevers, R., and Tank, D.W. (2017). Mapping of a non-spatial dimension by the
598 hippocampal-entorhinal circuit. Nature *543*, 719–722.
599 Battaglia, F.P., Benchenane, K., Sirota, A., Pennartz, C.M.A., and Wiener, S.I. (2011). The
600 hippocampus: hub of brain network communication for memory. Trends Cogn. Sci. *15*, 310–
601 318.
602 Chen, G., King, J.A., Burgess, N., and O'Keefe, J. (2013). How vision and movement combine
603 in the hippocampal place code. Proc. Natl. Acad. Sci. U. S. A. *110*, 378–383.
604 Cohen, J.Y., Haesler, S., Vong, L., Lowell, B.B., and Uchida, N. (2012). Neuron-type-specific
605 signals for reward and punishment in the ventral tegmental area. Nature *482*, 85–88.
606 Euston (2012). Role of mpfc. Changes *29*, 997–1003.
607 Funahashi, S., Chafee, M. V., and Goldman-Rakic, P.S. (1993). Prefrontal neuronal activity in
608 rhesus monkeys performing a delayed anti-saccade task. Nature *365*, 753–756.
609 Goldman-Rakic, P.. (1995). Cellular basis of working memory. Neuron *14*, 477–485.
610 Hattori, S., Chen, L., Weiss, C., and Disterhoft, J.F. (2015). Robust hippocampal responsivity
611 during retrieval of consolidated associative memory. Hippocampus *25*, 655–669.
612 Herzog, L.E., Katz, D.B., and Jadhav, S.P. (2020). Refinement and Reactivation of a Taste-
613 Responsive Hippocampal Network. Curr. Biol. *30*, 1306-1311.e4.
614 Jadhav, S.P., Rothschild, G., Roumis, D.K., and Frank, L.M. (2016). Coordinated Excitation and
615 Inhibition of Prefrontal Ensembles during Awake Hippocampal Sharp-Wave Ripple Events.
616 Neuron *90*, 113–127.
617 Joo, H.R., and Frank, L.M. (2018). The hippocampal sharp wave–ripple in memory retrieval
618 for immediate use and consolidation. Nat. Rev. Neurosci. *19*, 744–757.
619 Kaefer, K., Nardin, M., Blahna, K., and Csicsvari, J. (2020). Replay of Behavioral Sequences in
620 the Medial Prefrontal Cortex during Rule Switching. Neuron *106*, 154-165.e6.
621 Lisman, J.E., and Grace, A.A. (2005). The Hippocampal-VTA Loop: Controlling the Entry of
622 Information into Long-Term Memory. Neuron *46*, 703–713.
623 Lopes-dos-Santos, V., Ribeiro, S., and Tort, A.B.L. (2013). Detecting cell assemblies in large
624 neuronal populations. J. Neurosci. Methods *220*, 149–166.

Lovett-Barron, M., Kaifosh, P., Kheirbek, M.A., Danielson, N., Zaremba, J.D., Reardon, T.R., Turi, G.F., Hen, R., Zemelman, B. V., and Losonczy, A. (2014). Dendritic inhibition in the hippocampus supports fear learning. Science (80-.). *343*, 857–863.

McClelland, J.L., McNaughton, B.L., and O'Reilly, R.C. (1995). Why there are complementary learning systems in the hippocampus and neocortex: Insights from the successes and failures of connectionist models of learning and memory. Psychol. Rev. *102*, 419–457.

McEchron, M.D., and Disterhoft, J.F. (1997). Sequence of Single Neuron Changes in CA1 Hippocampus of Rabbits During Acquisition of Trace Eyeblink Conditioned Responses. J. Neurophysiol. *78*, 1030–1044.

McEchron, M.D., Bouwmeester, H., Tseng, W., Weiss, C., and Disterhoft, J.F. (1999). Hippocampectomy disrupts auditory trace fear conditioning and contextual fear conditioning in the rat. Hippocampus *8*, 638–646.

Nokia, M.S., Mikkonen, J.E., Penttonen, M., and Wikgren, J. (2012). Disrupting neural activity related to awake-state sharp wave-ripple complexes prevents hippocampal learning. Front. Behav. Neurosci. *6*, 84.

Ólafsdóttir, H.F., Bush, D., and Barry, C. (2018). The Role of Hippocampal Replay in Memory and Planning. Curr. Biol. *28*, R37–R50.

Otis, J.M., Namboodiri, V.M.K., Matan, A.M., Voets, E.S., Mohorn, E.P., Kosyk, O., McHenry, J.A., Robinson, J.E., Resendez, S.L., Rossi, M.A., et al. (2017). Prefrontal cortex output circuits guide reward seeking through divergent cue encoding. Nature *543*, 103–107.

Pachitariu, M., Steinmetz, N.A., Kadir, S.N., Carandini, M., and Harris, K.D. (2016). Fast and accurate spike sorting of high-channel count probes with KiloSort. 4448–4456.

Peyrache, A., Khamassi, M., Benchenane, K., Wiener, S.I., and Battaglia, F.P. (2009). Replay of rule-learning related neural patterns in the prefrontal cortex during sleep. Nat. Neurosci. *12*, 919–926.

Rothschild, G., Eban, E., and Frank, L.M. (2017). A cortical–hippocampal–cortical loop of information processing during memory consolidation. Nat. Neurosci. *20*, 251–259.

Roux, L., Hu, B., Eichler, R., Stark, E., and Buzsáki, G. (2017). Sharp wave ripples during learning stabilize the hippocampal spatial map. Nat. Neurosci. *20*, 845–853.

Rummell, B.P., Klee, J.L., and Sigurdsson, T. (2016). Attenuation of Responses to Self-Generated Sounds in Auditory Cortical Neurons. J. Neurosci. *36*, 12010–12026.

Schmidt-Hieber, C., and Häusser, M. (2013). Cellular mechanisms of spatial navigation in the

medial entorhinal cortex. Nat. Neurosci. *16*, 325–331.

Starkweather, C.K., Gershman, S.J., and Uchida, N. (2018). The Medial Prefrontal Cortex Shapes Dopamine Reward Prediction Errors under State Uncertainty. Neuron *98*, 616-629.e6.

Steinmetz, N.A., Zatka-Haas, P., Carandini, M., and Harris, K.D. (2019). Distributed coding of choice, action and engagement across the mouse brain. Nature *576*, 266–273.

Takehara-Nishiuchi, K., and McNaughton, B.L. (2008). Spontaneous changes of neocortical code for associative memory during consolidation. Science *322*, 960–963.

Takehara, K., Kawahara, S., and Kirino, Y. (2003). Time-dependent reorganization of the brain components underlying memory retention in trace eyeblink conditioning. J. Neurosci. *23*, 9897–9905.

Tang, W., Shin, J.D., Frank, L.M., and Jadhav, S.P. (2017). Hippocampal-prefrontal reactivation during learning is stronger in awake compared with sleep states. J. Neurosci. *37*, 11789–11805.

Taxidis, J., Pnevmatikakis, E.A., Dorian, C.C., Mylavarapu, A.L., Arora, J.S., Samadian, K.D., Hoffberg, E.A., and Golshani, P. (2020). Differential Emergence and Stability of Sensory and Temporal Representations in Context-Specific Hippocampal Sequences. Neuron.

Terada, S., Sakurai, Y., Nakahara, H., and Fujisawa, S. (2017). Temporal and Rate Coding for Discrete Event Sequences in the Hippocampus. Neuron *94*, 1248-1262.e4.

Supplementary Figures

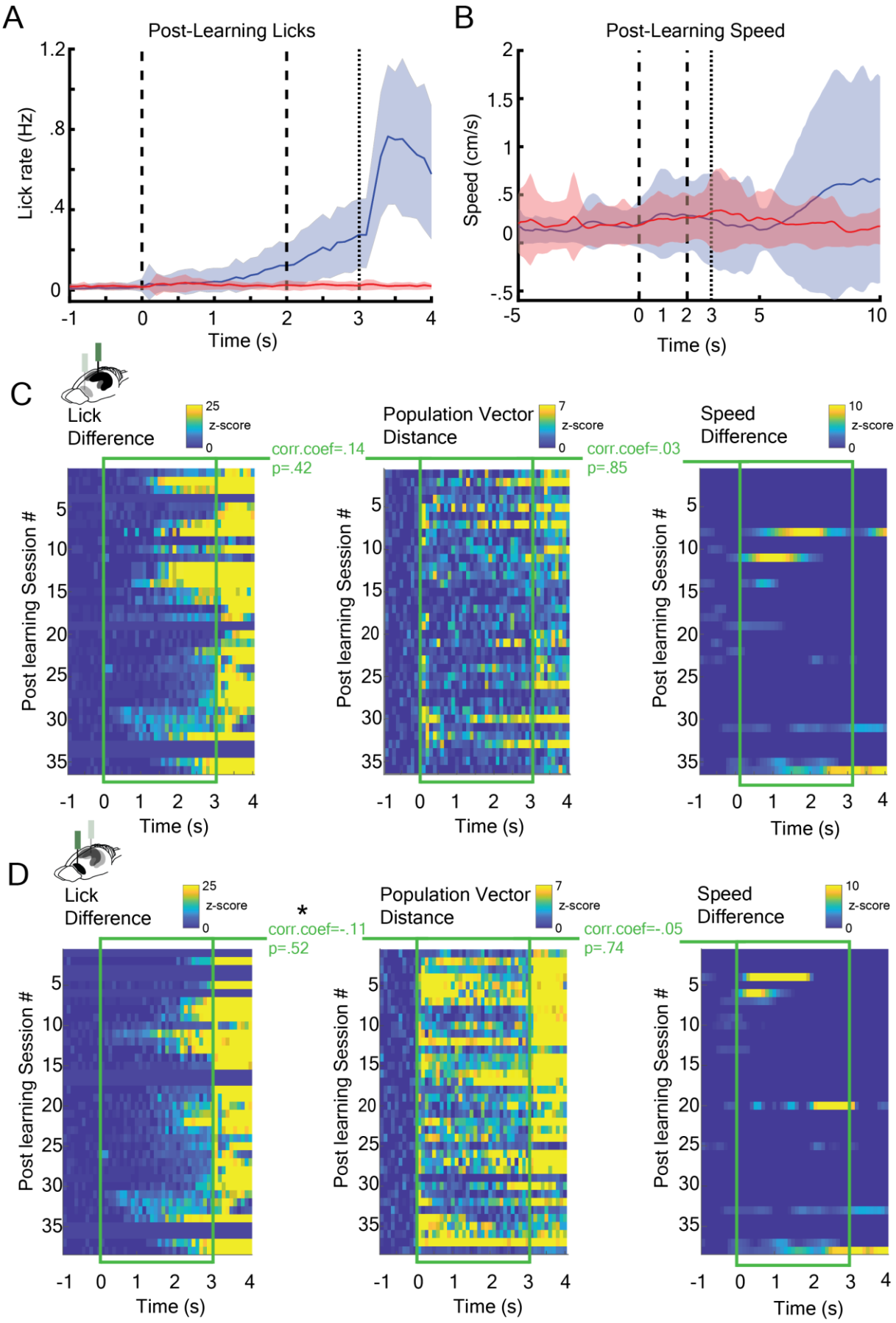

Supplementary Figure 1. *CA1 and PFC non-lick cell population activity does not correlate with lick or running behavior.* ***A)*** *Average Lick responses during post-learning trials for CS+ and CS- trials (52 sessions, 17 animals).* ***B)*** *Average running speed during post-learning CS+ and CS- trials (52 sessions, 17 animals).* ***C & D)*** *Correlation between non-lick population rate vector differences (CS+ vs CS- trials) for all post learning sessions in CA1 (C) and PFC (D) (middle) and differences in lick rate (CS+ vs CS- trials) (left) and differences in running Speed (CS+ vs CS- trials) (right) for all post learning sessions.*

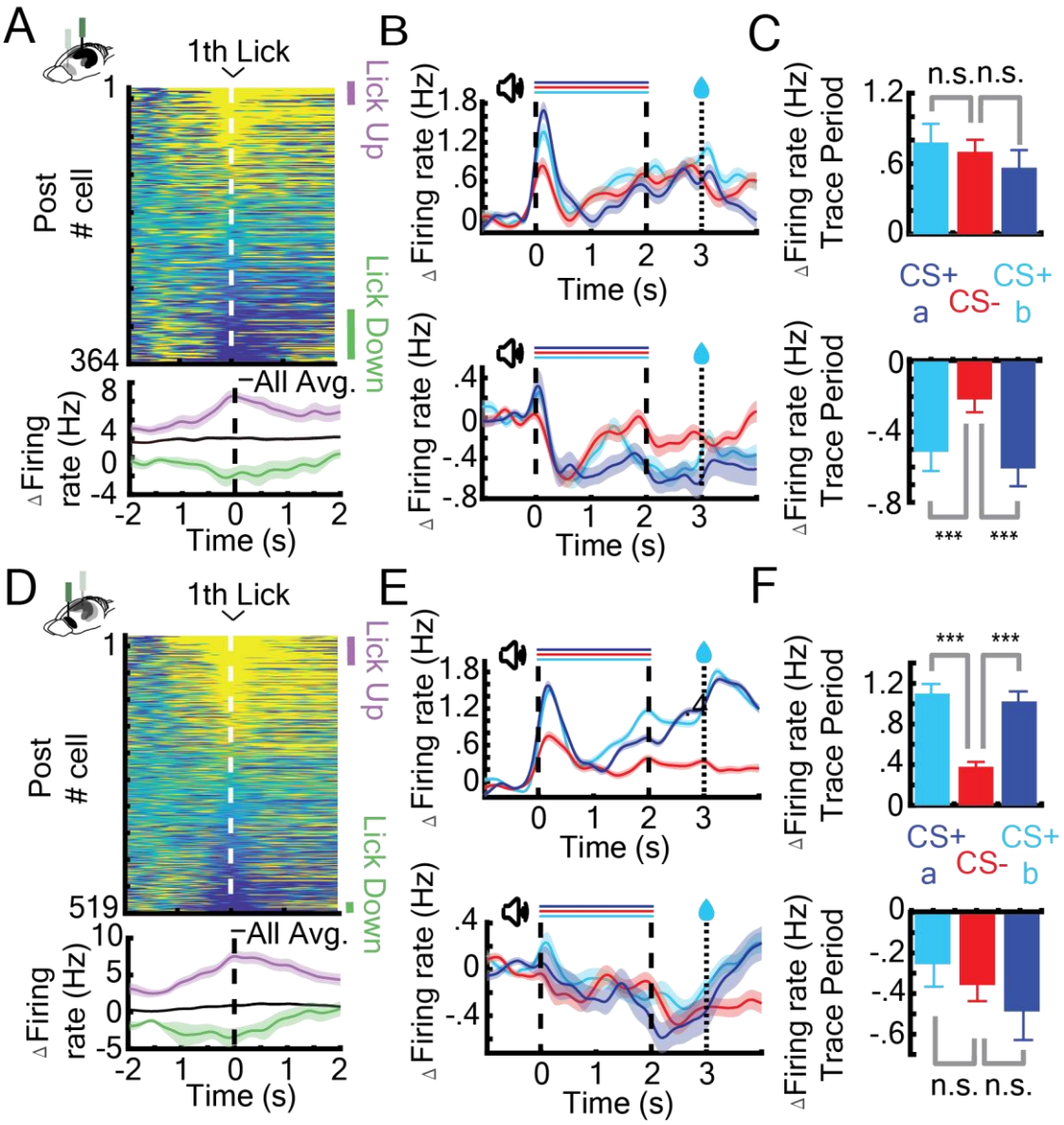

Supplementary Figure 2. *CA1 and PFC single cell is exhibit lick evoked and distinct patterns of sustained activity during the AATC2R task.* ***A & D****) Z-scored firing rates of all CA1 (A) and PFC (D) neurons (Top) aligned to the first lick of a lick bout (at least 3 licks/s) during CS+ trials (before reward delivery). Average change in activity of all, positively and negatively lick modulated cells (bottom). Purple and green bars indicate Lick Up and Lick Down cells that contributed to the averages.* ***B & E)*** *Average baseline-corrected PSTHs of all Trace-up (Top) and Trace-Down (Bottom) non-lick neurons during*

AATC2R task post learning for CA1 (B) (Trace up, n=202; Trace Down, n=239) and PFC (E) (Trace up, n=406; Trace Down, n=287). ***C & F)*** *Average mean change in firing rate during the trace period of the same Trace-Up neurons (Top) and Trace-Down neurons (bottom) as in B & E for CA1 and PFC (*** represent Wilcoxon rank sum, p<0.001 respectively, n.s = not significant).*